Available online at www.sciencedirect.com

Dyes and Pigments 71 (2006) 43–53

www.elsevier.com/locate/dyepig

Thermodynamics of anionic dye–cationic surfactant interactions in cationic–nonionic surfactant mixtures in comparison with binary systems

Barbara Simončič*, Mateja Kert

University of Ljubljana, Faculty of Natural Sciences and Engineering, Department of Textiles, Snežniška 5,
1000 Ljubljana, Slovenia

Received 7 January 2005; received in revised form 6 June 2005; accepted 15 June 2005

Abstract

The thermodynamics of the interactions between the anionic dye Acid Red 88 (AR88) and the cationic surfactant dodecyltrimethylammonium bromide (DTA) in the aqueous solution of the nonionic surfactant Triton X-100 (TX100) at different temperatures has been investigated by using potentiometry. The standard free energy change, ΔG_1°, the standard enthalpy change, ΔH_1°, and the standard entropy change, ΔS_1°, for the first association step of DTA–AR88 complex formation in the presence of TX100 micelles were determined and compared to the thermodynamic functions of DTA–AR88 and DTA–TX100 interactions in binary systems. From ΔG_1° results, it has been observed that irrespective of the studied temperature the binding free energy of DTA cation to AR88 anion as well as the complex stability is lower in TX100 solution than in binary mixture. The increase in the TX100 concentration causes the decrease in the tendency of DTA–AR88 complex formation. From this it can be seen that the mode and the strength of intermolecular interactions strongly depend on the presence of TX100 micelles. The values of ΔH_1° and ΔS_1° for DTA–AR88 complex formation in TX100 solution which are directly affected by the ratio of AR88 and TX100 concentrations are much higher compared to those obtained in binary mixtures without TX100. These results also lead to a conclusion that the binding of DTA cation to AR88 anion in the presence of TX100 micelles, which is an entropy-driven process, is much more different from the enthalpy-controlled formation process of DTA–AR88 complex in binary mixtures.

Keywords: Dye–surfactant interactions; Thermodynamics; Anionic dye; Cationic–nonionic surfactant mixtures; Potentiometry; Surfactant selective electrode

1. Introduction

In the theory of textile coloration, studies on dye–surfactant and surfactant–surfactant interactions in aqueous solutions represent the very important research topics. The complex formation processes between dyes and surfactants of different structures are investigated in binary mixtures [1–9] and in mixed surfactant systems [10–13]. Since in dyeing processes the mixtures of different surfactants are widely used, the interactions between ionic and nonionic surfactants which form mixed micelles are also of great interest [14–17].

In our previous paper [10], we presented the importance of the potentiometric method for the investigation of the dye–surfactant interactions in systems where cationic and nonionic surfactants are present in aqueous anionic dye solutions. We also applied an appropriate theoretical model for the quantitative study of these interactions [18]. Since we established that the nature of

---

* Corresponding author. Tel.: +386 1 200 32 31; fax: +386 1 200 32 70.
E-mail address: barbara.simoncic@ntf.uni-lj.si (B. Simončič).

doi:10.1016/j.dyepig.2005.06.013

interactions between anionic dyes and cationic surfactants in the presence of nonionic surfactant micelles very much differs from the one obtained in the absence of nonionic surfactant in the mixture, we continued with this research work in order to find out the reasons for the different mechanisms of intermolecular interactions in the studied systems.

In order to explain the nature of dye–surfactant interactions in two and three-component mixtures quantitatively, the thermodynamic aspects of the binding of cationic surfactant dodecyltrimethylammonium bromide to anionic dye C.I. Acid Red 88 with and without the presence of nonionic surfactant Triton X-100 had to be assessed. The standard free energy, enthalpy and entropy for the first association step of the formation of the anionic dye–cationic surfactant complex in the presence of nonionic surfactant micelles were determined and compared to the thermodynamic functions of the dye–surfactant and surfactant–surfactant interactions in binary systems.

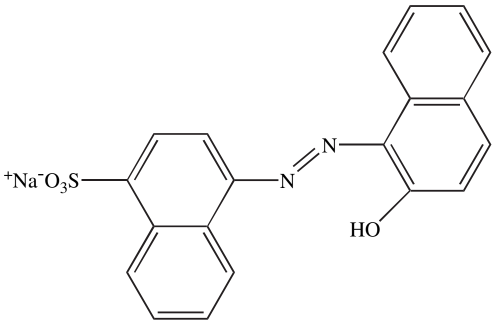

I

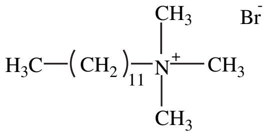

II

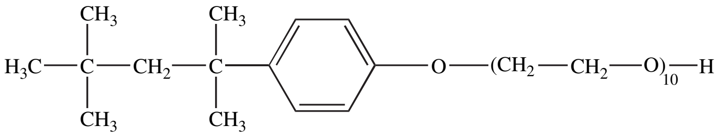

III

2. Experimental

2.1. Materials

The anionic azo dye C.I. Acid Red 88 (AR88, structure **I**), the cationic surfactant *n*-dodecyltrimethylammonium bromide (DTA, structure **II**) and the nonionic surfactant polyoxyethylene *tert*-octyl phenol, Triton X-100 (TX100, structure **III**) were Aldrich-Chemical Company's commercial products. AR88 was purified with the repeated recrystallization from aqueous acetone solution and from the *N,N′*-dimethylformamide–acetone. DTA was purified with three recrystallizations from acetone while TX100 was used without further purification. Sodium dodecylsulphate (SDS) (Aldrich-Chemical Co.), which was used for the preparation of the ion-exchange complex, was also purified by three recrystallizations from acetone. All solutions were prepared in double distilled water by weighing and expressed in molal concentrations.

2.2. Methods

2.2.1. Potentiometry

Potentiometric measurements, based on the use of DTA-selective membrane electrode, were carried out in the following electrode cell:

Ag | AgCl | reference solution; 1×10^{-4} mol/kg DTA + 0.1 mol/kg NaCl, | polymer membrane | test solution; m_S || KCl (satd.) | Hg_2Cl_2 | Hg.

Ion-selective membrane electrode was prepared by using a well-known method [19] and constructed in our laboratory [1,20]. The potentiometric method used was also described in detail in other publications [1,21].

The potentiometric measurements of e.m.f. (E) versus total concentration (m_S) of DTA were carried out in aqueous solutions with constant concentration of TX100 higher than c.m.c. [22] (5.0×10^{-3}, 1.0×10^{-2} and 5.0×10^{-2} mol/kg), or AR88 (5.0×10^{-5}, 1.0×10^{-4}, 5.0×10^{-4} and 1.0×10^{-3} mol/kg), or in mixtures of TX100 and AR88, in which the dye and surfactant concentrations mentioned above are used in combinations.

All solutions contain 5.0×10^{-3} mol/kg NaBr. The temperatures used were 15, 25, 35, and 45 °C.

3. Results and discussion

Fig. 1 shows the plots of E versus $\log m_S$ of DTA in 1.0×10^{-4} m AR88 and 1.0×10^{-2} m TX100 solutions as well as in AR88–TX100 mixtures of the same concentrations at four different temperatures. As it can be seen from the figure, the calibration curves which represent plots E versus m_S of DTA in water without added TX100 or AR88, are linear over the concentration range of 4.1×10^{-6}–8.8×10^{-3} mol/kg. In accordance with the Nernstian response [23] the slope of the linear plot was +57.0 mV/decade at 15 °C, +59.4 mV/decade at 25 °C, +61.0 mV/decade at 35 °C, and +62.7 mV/decade at 45 °C. All the titration curves, which represent plots of E versus $\log m_S$ of DTA obtained in DTA–TX100, DTA–AR88 and DTA–AR88–TX100 solutions, deviate from linearity over the whole concentration range measured. Since, this indicates that at any measured concentration of DTA the concentration of free surfactant cations, which can be detected by the DTA-selective electrode, is lower than the total concentration, m_S. The electrode is not sensitive to DTA bounded to dye–surfactant and surfactant–surfactant complexes.

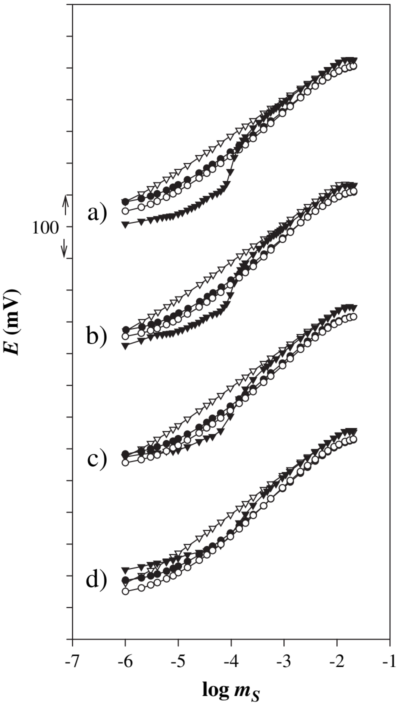

Fig. 1. Plots of e.m.f., E, of the cell versus the logarithm of the molal concentration, $\log m_S$, of DTA in TX100 and AR88 solutions at different temperatures (a) 15, (b) 25, (c) 35, (d) 45 °C. -▽-▽-: calibration curve, -●-●-: 1.0×10^{-2} mol/kg TX100, -▼-▼-: 1.0×10^{-4} mol/kg AR88, -○-○-: mixture of 1.0×10^{-2} mol/kg TX100 and 1.0×10^{-4} mol/kg AR88.

Calibration curve was obtained below the c.m.c of DTA, where linear behaviour is observed at any E measured value, the total DTA concentration, m_S, was obtained from the titration curve and the corresponding concentration, $m_{S,F}$ of free DTA cations from the calibration curve. The concentration of DTA cations from which the complexes were formed is equal to $(m_S - m_{S,F})$.

The formation of dye–surfactant and surfactant–surfactant complexes in the studied solutions can be described as a set of multiple equilibria:

$$S^+ + D^- \overset{K_1}{\leftrightarrow} DS \tag{1}$$

$$S^+ + DS \overset{K_2}{\leftrightarrow} DS_2^+ \tag{2}$$

...

$$S^+ + DS_{n-1}^{+(n-2)} \overset{K_n}{\leftrightarrow} DS_n^{+(n-1)} \tag{3}$$

and

$$S^+ + M \overset{\kappa_1}{\leftrightarrow} MS^+ \tag{4}$$

$$S^+ + MS^+ \overset{\kappa_2}{\leftrightarrow} MS_2^{2+} \tag{5}$$

...

$$S^+ + MS_{n-1}^{+(n-1)} \overset{\kappa_n}{\leftrightarrow} MS_n^{+n} \tag{6}$$

where S^+, D^- and M refer to the free DTA cation, the free AR88 anion and TX100 micelle, $DS_n^{+(n-1)}$ and MS_n^{+n} to complexes with different numbers of bound DTA cations, n, and $K_1, K_2, \ldots, K_n$ and $\kappa_1, \kappa_2, \ldots, \kappa_n$ are the corresponding stoichiometric equilibrium constants. In this theoretical approach it is assumed that only mononuclear complexes are formed in the studied mixtures. This is characteristic of a large number of systems, especially of diluted solutions [18].

Since the concentration of free DTA cations as a function of the total concentrations of DTA, AR88 and TX100 is obtained as a result of the potentiometric measurements, the quantity of complex formation can be expressed as the degree of binding, β. In this case the average number of DTA cations bound to each AR88 anion, β_D, or TX100 micelle, β_M, can be calculated properly from the relationships [18]:

$$\beta_D = \frac{m_S - m_{S,F}}{m_D} \tag{7}$$

and

$$\beta_M = \frac{m_S - m_{S,F}}{m_M} \tag{8}$$

where $m_{S,F}$ is the concentration of free DTA cations, m_D is the total concentration of AR88 and m_M is the total concentration of the TX100 micelle which equals to $(m_N - \text{c.m.c.})/\nu$; m_N represents the stoichiometric concentration of TX100 and ν its micellar aggregation number [24]. Since in the case of multiple equilibria (1)–(6) the concentrations of complexes can be expressed by free DTA concentration and the association constants, the degree of binding, β, of Eqs. (7) and (8) can be written as:

$$\beta_D = \frac{K_1 m_{S,F} + 2K_1K_2m_{S,F}^2 + \cdots + nK_1K_2\ldots K_n m_{S,F}^n}{1 + K_1 m_{S,F} + K_1K_2m_{S,F}^2 + \cdots + K_1K_2\ldots K_n m_{S,F}^n} \tag{9}$$

$$\beta_M = \frac{\kappa_1 m_{S,F} + 2\kappa_1\kappa_2m_{S,F}^2 + \cdots + n\kappa_1\kappa_2\ldots \kappa_n m_{S,F}^n}{1 + \kappa_1 m_{S,F} + \kappa_1\kappa_2m_{S,F}^2 + \cdots + \kappa_1\kappa_2\ldots \kappa_n m_{S,F}^n} \tag{10}$$

where it is considered that each mole of a complex includes n moles of bound DTA.

In the solutions which contain all three components DTA, AR88 and TX100 and considering the experimental conditions that were used, it can be assumed that DTA cations form complexes with both species, dye anions and TX100 micelles. Therefore, the concentration of bound DTA cations, which can be obtained by the potentiometric measurements, consists of two contributions – the first due to DTA binding to AR88 and the second due to DTA binding to TX100 micelles. Since use, the measurements of E versus m_S of DTA were done in the TX100 solution, in the presence as well as in the absence of AR88, the difference between the deviations of the potentiometric curves from the calibration curve at any stoichiometric concentration is a measure of the concentration of DTA cations bound to AR88 anions in the TX100 solution. According to this use, the degree of binding of DTA cations to AR88 anions, β_D, in the presence of TX100 micelles can be calculated as follows:

$$\beta_D = \frac{m_S - m_{S,F} - \beta_M m_M}{m_D} \tag{11}$$

For the systems where the DTA binding process increases progressively with increased DTA concentration, the equilibrium constant K_1 for the DS complex formation between DTA and AR88, and κ_1 for the MS^+ complex formation between DTA and TX100 micelle in the equilibria (1) and (4) can be calculated from the Eqs. (9)–(11) as follows [18,25]:

$$\lim_{m_{S,F}\to 0}\frac{\beta_D}{m_{S,F}} = K_1; \quad \lim_{m_{S,F}\to 0}\frac{\beta_M}{m_{S,F}} = \kappa_1 \tag{12}$$

If the values of $\beta_D/m_{S,F}$ and $\beta_M/m_{S,F}$ are plotted against $m_{S,F}$, the values K_1 and κ_1 are obtained by the extrapolation to zero free DTA concentration. Representative results are shown in Fig. 2. The values of K_1 and κ_1 for DTA–AR88, DTA–TX100 and DTA–AR88–TX100 systems are summarised in Tables 1–3.

From the values obtained for K_1 and κ_1 at different temperatures (Tables 1–3), the standard free energy change, ΔG_1^o, the standard enthalpy change, ΔH_1^o, and the standard entropy change, ΔS_1^o, for the formation of SD and MS^+ complexes in the first step in multiple equilibria (1) and (4) can be calculated as follows [26]:

$$\Delta G_1^o = -RT\ln K_1; \quad \Delta G_1^o = -RT\ln \kappa_1 \tag{13}$$

$$\Delta H_1^o = \frac{\partial\left(\Delta G_1^o/T\right)}{\partial(1/T)} \tag{14}$$

$$\Delta S_1^o = \frac{\Delta H_1^o - \Delta G_1^o}{T} \tag{15}$$

It can be seen from Eq. (14) that if $\Delta G_1^o/T$ is plotted against $1/T$, the slope of the curve at any temperature is equal to ΔH_1^o at that temperature. But, if we assume that ΔH_1^o does not depend on the temperature over the measured temperature range, a plot of $\Delta G_1^o/T$ versus $1/T$ should be a straight line with a slope equal to ΔH_1^o. These plots are shown in Figs. 3 and 4. The thermodynamic quantities are summarised in Tables 1–3.

For the DS complex formation between AR88 and DTA in the equilibrium (1), with and without TX100, the free energy change can be expressed as:

$$\Delta G_1 = \Delta G_1^o + RT\ln\frac{m_{DS}}{m_{D,F}m_{S,F}} \tag{16}$$

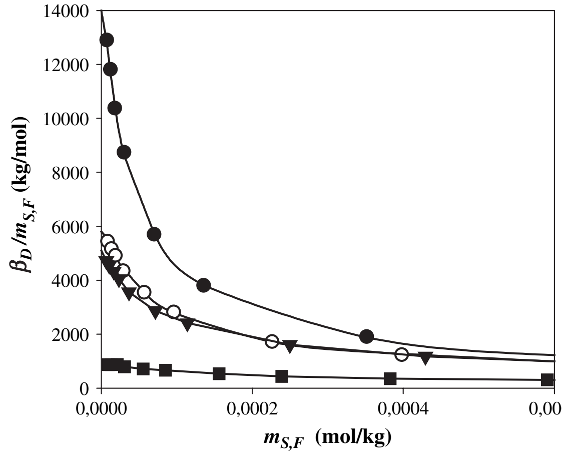

Fig. 2. Plots of values of $\beta_D/m_{S,F}$ versus the DTA free cation concentration $m_{S,F}$, obtained in mixtures of AR88 and TX100 of different concentrations. -●-●-: 5.0×10^{-3} mol/kg TX100 and 5.0×10^{-4} mol/kg AR88 at 25 °C, -○-○-: 1.0×10^{-2} mol/kg TX100 and 5.0×10^{-4} mol/kg AR88 at 25 °C, -▼-▼-: 1.0×10^{-2} mol/kg TX100 and 5.0×10^{-4} mol/kg AR88 at 15 °C, -■-■-: 5.0×10^{-2} mol/kg TX100 and 5.0×10^{-4} mol/kg AR88 at 25 °C.

Table 1
Association constants, K_1, and thermodynamic functions of DTA–AR88 complex formation ($S^+ + D^- \leftrightarrow SD$) at different temperatures

m_D (mol/kg)	T (°C)	$K_1 \times 10^{-4}$	ΔG_1^o (kJ/mol)	ΔH_1^o (kJ/mol)	ΔS_1^o (J/mol K)	ΔG_{el}^o (kJ/mol)	ΔG_{mix}^o (kJ/mol)	ΔG_{sr}^o (kJ/mol)	ΔH_{sr}^o (kJ/mol)	ΔS_{sr}^o (J/mol K)
5×10^{-5}	15	13.0	−28.2	−42.0 ± 0.6	−47.9	−4.7	9.6	−33.1	−43.5	−36.3
	25	8.0	−28.0		−47.1	−5.0	10.0	−33.0	−43.8	−36.5
	35	5.5	−27.9		−45.6	−5.2	10.3	−33.0	−44.2	−36.1
	45	2.4	−26.7		−48.2	−5.4	10.6	−31.8	−44.5	−39.8
1×10^{-4}	15	23.0	−29.6		−43.2	−4.7	9.6	−34.4	−43.5	−31.6
	25	13.0	−29.2		−43.0	−5.0	10.0	−34.2	−43.8	−32.4
	35	8.5	−29.1		−42.0	−5.2	10.3	−34.2	−44.2	−32.5
	45	3.3	−27.5		−45.6	−5.4	10.6	−32.7	−44.5	−37.2
5×10^{-4}	15	38.0	−30.8		−39.0	−4.7	9.6	−35.6	−43.5	−27.4
	25	24.0	−30.7		−37.9	−5.0	10.0	−35.7	−43.8	−27.3
	35	13.0	−30.2		−38.5	−5.2	10.3	−35.2	−44.2	−28.9
	45	7.4	−29.6		−38.9	−5.4	10.6	−34.8	−44.5	−30.5
1×10^{-3}	15	50.0	−31.4		−36.7	−4.7	9.6	−36.3	−43.5	−25.1
	25	30.0	−31.2		−36.1	−5.0	10.0	−36.2	−43.8	−25.5
	35	19.0	−31.1		−35.3	−5.2	10.3	−36.2	−44.2	−25.8
	45	9.0	−30.2		−37.2	−5.4	10.6	−35.3	−44.5	−28.9

where m_{DS} represents the concentration of complex and $m_{D,F}$ the concentration of free AR88 anions. In Eq. (16) the term which includes activity coefficients is neglected because the concentrations of the solutions are very low.

On the other hand, at low concentrations ΔG_1 can be expressed in terms of mole fractions of the dye anions, $X_{D,F}$, the surfactant cations, $X_{S,F}$, and the complex, X_{DS}, as follows:

$$\Delta G_1 = \Delta G_u^o + RT \ln \frac{X_{DS}}{X_{D,F} X_{S,F}} \qquad (17)$$

where ΔG_u^o is the standard unitary free energy for the DS complex formation.

At very low concentrations of the surfactant and the dye the sum of $n_{D,F}$ moles of the dye anions, $n_{S,F}$ moles of the surfactant cations and n_{DS} moles of the DS complexes is much lower than n_w moles of water. In this case the mole fractions $X_{D,F}$, $X_{S,F}$ and X_{DS} can be written as $n_{D,F}/n_w$, $n_{S,F}/n_w$ and n_{DS}/n_w, respectively. Since, the molal concentrations m_D, m_S and m_{DS} can be substituted for n_D, n_S and n_{DS} in Eq. (17). For the same reason n_w is equal to $1000/M_w = 55.6$ and written as $1/M_0$. Taking all this into consideration, Eq. (17) can be written as:

$$\Delta G_1 = \Delta G_u^o + RT \ln \frac{m_{DS}}{m_D m_S} - RT \ln M_0 \qquad (18)$$

From Eqs. (17) and (18) it follows that:

$$\Delta G_1^o = \Delta G_u^o - RT \ln M_0 \qquad (19)$$

where $-RT \ln M_0 = \Delta G_{mix}^o$, i.e. the standard free energy of mixing which represents the contribution from the random mixing of dye and surfactant ions with water, when dye and surfactant ions transform to DS complex.

Table 2
Association constants, κ_1, and thermodynamic functions of DTA–TX100 micelle complex formation ($S^+ + M \leftrightarrow MS^+$) at different temperatures

m_N (mol/kg)	T (°C)	$\kappa_1 \times 10^{-4}$ (mol/kg)	ΔG_1^o (kJ/mol)	ΔH_1^o (kJ/mol)	ΔS_1^o (J/mol K)	ΔG_{sr}^o (kJ/mol)	ΔS_{sr}^o (J/mol K)
5×10^{-3}	15	1.8	−23.5	4.3 ± 0.6	96.4	−33.1	129.8
	25	2.3	−24.9		97.9	−34.8	131.3
	35	1.9	−25.2		95.9	−35.5	129.3
	45	2.4	−26.7		97.4	−37.3	130.8
1×10^{-2}	15	2.6	−24.3		99.4	−34.0	132.9
	25	3.0	−25.6		100.1	−35.5	133.5
	35	3.3	−26.6		100.5	−36.9	133.9
	45	2.9	−27.2		98.9	−37.7	132.4
5×10^{-2}	15	2.9	−24.6		100.4	−34.2	133.8
	25	3.7	−26.1		101.9	−36.0	135.3
	35	3.7	−27.0		101.4	−37.2	134.8
	45	3.6	−27.7		100.7	−38.4	134.1

Table 3
Association constants, K_1, and thermodynamic functions of DTA–AR88 complex formation ($S^+ + D^- \leftrightarrow SD$) in the presence of TX100 at different temperatures

m_N (mol/kg)	m_D (mol/kg)	T (°C)	$K_1 \times 10^{-3}$	ΔG_1^o (kJ/mol)	ΔH_1^o (kJ/mol)	ΔS_1^o (J/mol K)	ΔG_{sr}^o (kJ/mol)	ΔH_{sr}^o (kJ/mol)	ΔS_{sr}^o (J/mol K)
5×10^{-3}	5×10^{-5}	15	7.0	−21.2	3.8	86.8	−26.1	2.3	98.4
		25	4.7	−20.9		83.0	−25.9	2.0	93.6
		35	6.5	−22.5		85.3	−27.6	1.6	94.9
		45	7.5	−23.6		86.1	−28.8	1.3	94.5
	1×10^{-4}	15	8.5	−21.7	−0.3	74.2	−26.5	−1.8	85.8
		25	7.1	−22.0		72.7	−27.0	−2.1	83.3
		35	7.0	−22.7		72.6	−27.8	−2.5	82.2
		45	8.5	−23.9		74.3	−29.1	−2.8	82.7
	5×10^{-4}	15	15.0	−23.0	−1.3	75.4	−27.9	−2.8	87.0
		25	14.0	−23.7		75.0	−28.6	−3.1	85.6
		35	12.0	−24.1		73.9	−29.1	−3.5	83.4
		45	15.0	−25.4		75.9	−30.6	−3.8	84.2
	1×10^{-3}	15	26.0	−24.3	−7.3	59.2	−29.2	−8.8	70.8
		25	20.0	−24.5		57.8	−29.5	−9.1	68.5
		35	23.0	−25.7		60.0	−30.8	−9.5	69.4
		45	18.0	−25.9		58.5	−31.1	−9.8	67.0
1×10^{-2}	5×10^{-5}	15	5.0	−20.4	11.4	110.4	−25.3	9.9	122.0
		25	2.4	−19.3		103.0	−24.3	9.6	113.6
		35	3.5	−20.9		104.9	−26.0	9.2	114.4
		45	7.5	−23.6		110.0	−28.8	8.9	118.4
	1×10^{-4}	15	5.5	−20.6	3.1	82.4	−25.5	1.6	94.0
		25	4.2	−20.7		79.8	−25.7	1.3	90.4
		35	5.0	−21.8		80.9	−26.9	0.9	90.4
		45	6.0	−23.0		82.1	−28.2	0.6	90.5
	5×10^{-4}	15	5.0	−20.4	2.7	80.2	−25.3	1.2	91.8
		25	5.7	−21.4		81.0	−26.4	0.9	91.6
		35	6.0	−22.3		81.1	−27.4	0.5	90.6
		45	5.5	−22.8		80.1	−28.0	0.2	88.5
	1×10^{-3}	15	7.0	−21.2	1.1	77.4	−26.1	−0.4	89.0
		25	7.0	−21.9		77.3	−26.9	−0.7	87.9
		35	8.0	−23.0		78.3	−28.1	−1.1	87.8
		45	7.0	−23.4		77.1	−28.6	−1.4	85.5
5×10^{-2}	5×10^{-5}	15	2.3	−18.5					
		25	1.8	−18.6					
		35	5.3	−22.0					
		45	/	/					
	1×10^{-4}	15	2.2	−18.4					
		25	1.6	−18.3					
		35	2.5	−20.0					
		45	/	/					
	5×10^{-4}	15	1.0	−16.5	0.1	57.8	−21.4	−1.4	69.4
		25	0.9	−16.9		56.9	−21.8	−1.7	67.5
		35	1.7	−19.0		62.2	−24.1	−2.1	71.7
		45	0.8	−17.7		55.9	−22.9	−2.4	64.3
	1×10^{-3}	15	1.1	−16.8	−1.5	53.0	−21.7	−3.0	64.6
		25	0.95	−17.0		52.0	−22.0	−3.3	62.6
		35	1.2	−18.2		54.1	−23.3	−3.7	63.6
		45	0.95	−18.1		52.3	−23.3	−4.0	60.7

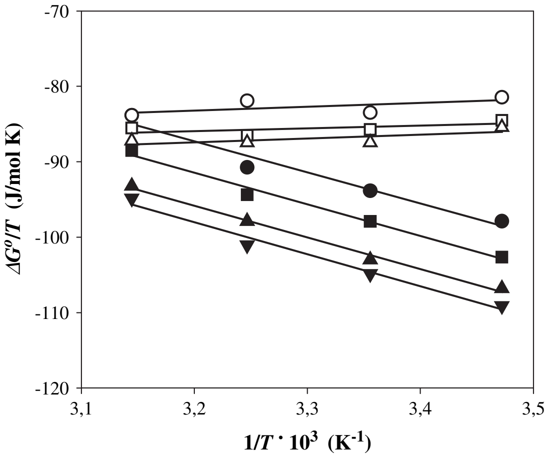

Fig. 3. Plots of $\Delta G_1^o/T$ versus $1/T$ for the first step of the DTA–AR88 and DTA–TX100 micelle complexes formation in binary mixtures of different concentrations. -●-●-: 5.0×10^{-5} mol/kg AR88, -■-■-: 1.0×10^{-4} mol/kg AR88, -▲-▲-: 5.0×10^{-4} mol/kg AR88, -▼-▼-: 1.0×10^{-3} mol/kg AR88, -○-○-: 5.0×10^{-3} mol/kg TX100, -□-□-: 1.0×10^{-2} mol/kg TX100, -△-△-: 5.0×10^{-2} mol/kg TX100.

Differentiation of ΔG_1^o with respect to temperature gives ΔS_1^o:

$$\Delta S_1^o = \Delta S_u^o + R \ln M_0 \tag{20}$$

In Eq. (20) ΔS_u^o is unitary entropy, which represents the contribution to the entropy due to dye–solvent and surfactant–solvent interactions [27,28].

The standard free energy change, ΔG_1^o, can be represented by three contributions:

$$\Delta G_1^o = \Delta G_{el}^o + \Delta G_{mix}^o + \Delta G_{sr}^o \tag{21}$$

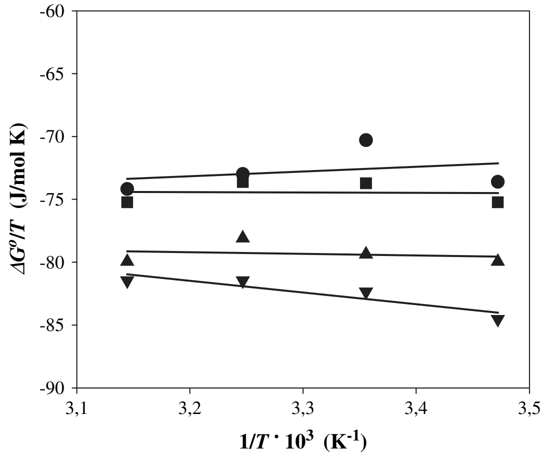

Fig. 4. Plots of $\Delta G_1^o/T$ versus $1/T$ for the first step of the DTA–AR88 complex formation in TX100 solutions of different compositions. -●-●-: 5.0×10^{-3} mol/kg TX100 and 5.0×10^{-5} mol/kg AR88, -■-■-: 5.0×10^{-3} mol/kg TX100 and 1.0×10^{-4} mol/kg AR88, -▲-▲-: 5.0×10^{-3} mol/kg TX100 and 5.0×10^{-4} mol/kg AR88, -▼-▼-: 5.0×10^{-3} mol/kg TX100 and 1.0×10^{-3} mol/kg AR88.

where ΔG_{el}^o is the electrostatic contribution resulting from Coulombic interactions. Furthermore, ΔG_{sr}^o contains the contributions of all attractive short range non-Coulombic interactions. In the first approximation ΔG_{el}^o can be expressed as:

$$\Delta G_{el}^o = -\frac{N_A e_0^2}{4\pi\varepsilon_o \varepsilon a} \tag{22}$$

where N_A is Avogadro's constant, e_0 is the charge, a is the average separation between charges in the complex, ε_o is the permittivity of vacuum and ε the dielectric constant of solvent. For a we took 3.57×10^{-10} m at 25 °C [29]. The values of ΔG_{el}^o were calculated from Eq. (22) and of ΔG_{sr}^o from Eq. (21).

Since in very dilute solutions ΔH_{mix}^o is equal to zero, it follows:

$$\Delta H_{sr}^o = \Delta H_1^o - \left(\Delta G_{el}^o + T\Delta S_{el}^o\right) \tag{23}$$

ΔS_{el}^o is obtained from the following equation [30]:

$$\Delta S_{el}^o = -\frac{d(\Delta G_{el})}{dT} = \Delta G_{el}^o \frac{d\ln(\varepsilon)}{dT} \tag{24}$$

where $d(\ln\varepsilon)/dT$ is equal to -4.6×10^{-3} K^{-1} at 25 °C [30,31].

Finally, the standard entropy change of short range interactions is:

$$\Delta S_{sr}^o = \frac{\left(\Delta H_{sr}^o - \Delta G_{sr}^o\right)}{T} \tag{25}$$

All the thermodynamic functions of the DTA–AR88 complex formation calculated from the equations described above are summarised in Tables 1 and 3.

In the mixtures of 5.0×10^{-2} m TX100 and 5.0×10^{-5} m AR88 or 5.0×10^{-2} m TX100 and 1.0×10^{-4} m AR88 at 45 °C, the differences between titration curves obtained in the presence and in the absence of AR88 were very small which prevent us to calculate the degree of binding of DTA cations to AR88 anions in the presence of TX100 micelles with the subtraction of the curves (Eq. (11)). As a result of this the values of K_1 and ΔG_1^o could not be determined for these systems (Table 3). Since only three values of ΔG_1^o are not enough for the graphical determination of ΔH_1^o from the van't Hoff law (Eq. (14)), the other values of thermodynamic functions could neither be calculated.

For the MS^+ complex formation between DTA and TX100 micelle in the equilibrium (4) we use the same thermodynamic treatment as for the DS complex formation. The only difference from the binding of DTA cation to AR88 anion is that for the binding process of DTA cation to TX100 micelle, there are no electrostatic interactions involved. In this case Eqs. (21) and (23) can be written in forms:

$$\Delta G^{\mathrm{o}}_{\mathrm{sr}} = \Delta G^{\mathrm{o}}_{1} - \Delta G^{\mathrm{o}}_{\mathrm{mix}} \tag{26}$$

$$\Delta H^{\mathrm{o}}_{\mathrm{sr}} = \Delta H^{\mathrm{o}}_{1} \tag{27}$$

while Eq. (25) remains unchanged. The corresponding thermodynamic functions are brought together in Table 2.

To be able to discuss the nature and the thermodynamics of dye–surfactant interactions in three-component mixtures, which consist of the dye AR88 and the surfactants DTA and TX100 of different concentrations, as well as the influence of TX100 micelles on the strength of DTA–AR88 interactions, it is necessary to first analyse the binding processes of DTA to AR88 and DTA to TX100 micelles in binary systems into the details.

The comparison of the results presented in Tables 1 and 2 shows that the values of thermodynamic functions differ in magnitude and in sign. These results confirm our previous investigations [14,32] that the dye–surfactant interactions take place in different way as the surfactant–surfactant interactions. The values of K_1, which are greater than those obtained for κ_1 show that the strength of the interactions in DTA–AR88 complex is stronger than in the complex between DTA and TX100 micelle in all studied conditions. It is seen from Table 1 that the values of K_1 not only change with temperature, but also with the initial concentration of AR88. The latter one is attributed to the change in ionic strength of the solution caused by DTA–AR88 complex formation, when the measurements are not made in the presence of a large excess of the electrolyte. The same results are obtained in the literature, where the binding processes are studied by conductometric or potentiometric titrations [33–35].

The standard free energy change, $\Delta G^{\mathrm{o}}_{1}$, which is in direct correlation with association constants K_1 and κ_1, also indicates the tendency of complex formation which is supported by the decrease in free energy. By comparing the values of $\Delta G^{\mathrm{o}}_{1}$ for DTA–AR88 complex formation to the values of $\Delta G^{\mathrm{o}}_{1}$ for DTA–TX100 complex formation, we can find out that complexes between DTA cations and AR88 anions form more willingly than complexes between DTA cations and TX100 micelles in the studied systems. Since by increasing the temperature, $\Delta G^{\mathrm{o}}_{1}$ decreases for DTA–AR88 complex formation which indicates that the complex formation is unfavourable, while the opposite has been observed for DTA–TX100. For DTA–AR88 complex formation, there are three contributions to $\Delta G^{\mathrm{o}}_{1}$, $\Delta G^{\mathrm{o}}_{\mathrm{el}}$, $\Delta G^{\mathrm{o}}_{\mathrm{mix}}$ and $\Delta G^{\mathrm{o}}_{\mathrm{sr}}$, while for DTA–TX100 only two contributions, $\Delta G^{\mathrm{o}}_{\mathrm{mix}}$ and $\Delta G^{\mathrm{o}}_{\mathrm{sr}}$, are present. It can be seen from Table 1 that Coulombic term $\Delta G^{\mathrm{o}}_{\mathrm{el}}$ for DTA–AR88 interactions is negative at all studied temperatures, indicating that electrostatic interactions between DTA cations and AR88 anions favour the dye–surfactant complex formation. $\Delta G^{\mathrm{o}}_{\mathrm{mix}}$, which includes solute–solvent interactions, has the same positive value of 9.6–10.6 kJ/mol for both studied interactions. This contribution is opposed by the formation of complexes DTA–AR88 and DTA–TX100 micelle. For both binding processes of DTA to AR88 and to TX100 the main contribution to the value of $\Delta G^{\mathrm{o}}_{1}$ is represented by $\Delta G^{\mathrm{o}}_{\mathrm{sr}}$. This contribution, which is composed of all attractive non-Coulombic interactions, includes dispersive, charge transfer and hydrophobic interactions. It can also be seen from the results that the values of $\Delta G^{\mathrm{o}}_{\mathrm{sr}}$ obtained for DTA–AR88 complex formation are very similar to those obtained for the DTA–TX100. It should be emphasized at the same time that the similarity in $\Delta G^{\mathrm{o}}_{\mathrm{sr}}$ values does not mean that the intermolecular forces which predominate in DTA–AR88 are the same as those in DTA–TX100 complexes. Due to the fact that it is not possible to separate the contributions of $\Delta G^{\mathrm{o}}_{\mathrm{sr}}$, intermolecular forces could be estimated only qualitatively in connection with the values of $\Delta S^{\mathrm{o}}_{1}$ and $\Delta H^{\mathrm{o}}_{1}$ for both the systems.

It can be seen from Tables 1 and 2 that the DTA–AR88 complex formation is accompanied by the negative values of $\Delta S^{\mathrm{o}}_{1}$ and $\Delta S^{\mathrm{o}}_{\mathrm{sr}}$, the high positive values of $\Delta S^{\mathrm{o}}_{1}$ and $\Delta S^{\mathrm{o}}_{\mathrm{sr}}$ were obtained for the DTA–TX100 complex formation. The positive value of $\Delta S^{\mathrm{o}}_{1}$ for DTA–TX100 complex formation shows that the system becomes more random after the transfer of a DTA cation from the aqueous bulk phase into the TX100 micelle, and the negative value of $\Delta S^{\mathrm{o}}_{1}$ for DTA–AR88 complex formation clearly indicates that the binding of a DTA cation to AR88 anion causes an increase in the order of the system. The difference in a sign of $\Delta S^{\mathrm{o}}_{\mathrm{sr}}$ values for the studied binding processes, can be interpreted in terms of two opposing contributions. The first one, which can be attributed to the disruption of the hydrophobically structured water around DTA cations and AR88 anions, which occurs when DTA binds to AR88 or to TX100 micelle, favours the complex formation and thus gives a positive contribution to $\Delta S^{\mathrm{o}}_{\mathrm{sr}}$. The second contribution, which is opposed to the complex formation and thus gives a negative contribution to $\Delta S^{\mathrm{o}}_{\mathrm{sr}}$, is the result of the loss of the rotational and translational entropy that accompanies the complex formation. While the first contribution obviously prevails in DTA–TX100 complex formation, the second one is the one which prevails in DTA–AR88 complex formation.

Furthermore, a great difference between the $\Delta H^{\mathrm{o}}_{1}$ values of DTA–AR88 and DTA–TX100 binding processes was also obtained. The negative value of $\Delta H^{\mathrm{o}}_{1}$, which is equal to -42.0 ± 0.7 kJ/mol for DTA–AR88 complex formation, indicates that this process is exothermic. On the other hand, the positive value of $\Delta H^{\mathrm{o}}_{1}$

equal to +4.3 ± 0.7 kJ/mol means that the DTA–TX100 association process is endothermic. The results also show that the endothermic contribution due to hydrophobic interactions, which results from the disruption of the hydrophobically structured water around the DTA cations when the binding process takes place, prevails in DTA–TX100 complex formation, this contribution has little effect on the value of ΔH_1^{o} in DTA–AR88 complex formation. The main contribution to the enthalpy of DTA to AR88 binding process is obviously the result of the dispersive interactions. Taking all these thermodynamic quantities into consideration, it can be concluded that the binding of DTA cation to AR88 anion is enthalpy-driven process and the binding of DTA cation to TX100 micelle is entropy-driven process.

By comparing the results in Table 3, which were obtained for DTA–AR88 interactions in TX100 solution of different concentrations, to those of binary mixtures in Tables 1 and 2, it can be seen that the values of thermodynamic functions for the DTA–AR88 interactions in TX100 solutions are much more different from those obtained in binary mixtures without TX100 at the same conditions. It means that the presence of TX100 micelles strongly affects the tendency of DTA–AR88 complex formation as well as the complex stability. The reason for this is a change in environment, when TX100 is added in the mixture of DTA and AR88. Much lower values of ΔG_1^{o} and $\Delta G_{\mathrm{sr}}^{\mathrm{o}}$ for DTA–AR88 complex formation in TX100 solution compared to those obtained in binary mixtures suggest that the binding energy of DTA cation to AR88 anion is lower in the presence of TX100 than in the absence of TX100 irrespective of the studied temperature. It is also clearly seen from Fig. 5 that at all studied temperatures the tendency of DTA–AR88 complex formation increases with the increase of AR88 concentration in TX100 solution of the lowest used concentration, and that the increase in the TX100 concentration causes a decrease in the DTA–AR88 association tendency, although the concentration of AR88 is increased. These results show that attractive forces between DTA cations and TX100 micelles as well as between AR88 anions and TX100 micelles create a counter-balancing mechanism against DTA–AR88 attractive forces. In the studied system, the addition of the surfactant TX100 highly decreases the c.m.c. of the surfactant mixture which strongly affects the binding process of DTA to AR88 and the DTA to TX100.

The values of ΔH_1^{o} and ΔS_1^{o} for DTA–AR88 complex formation in TX100 solution (Table 3) are also surprisingly unexpected. They are much higher compared to those obtained in binary mixtures without TX100 (Table 1) and they are also directly affected by the AR88/TX100 concentration ratio. Since the value of ΔH_1^{o} decreases with the increase in the AR88 concentration at constant TX100 concentration, the increase in TX100 concentration results in the increase of the ΔH_1^{o} value at constant concentration of AR88. These changes in ΔH_1^{o} values are most likely caused by the changes in the size of its contributions due to hydrophobic and dispersive interactions. It also indicates that the interaction process has a tendency to convert from endothermic to exothermic by increasing AR88 concentration and that the binding process becomes more endothermic when the TX100 concentration is increased. The high positive values of ΔS_1^{o} and $\Delta S_{\mathrm{sr}}^{\mathrm{o}}$ for DTA–AR88 complex formation in TX100 solution, which are much more similar to those obtained for DTA–TX100 interactions than to those obtained for DTA–AR88 in binary systems (Fig. 6), suggest that

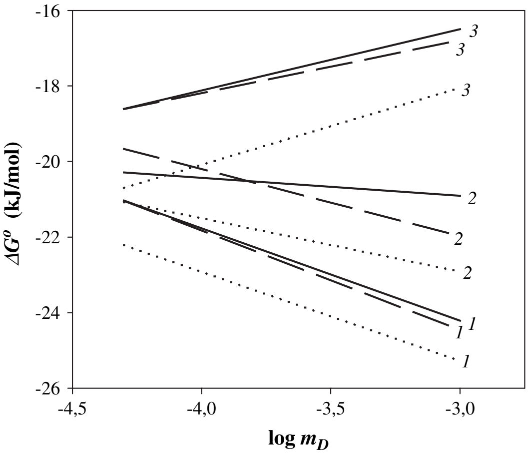

Fig. 5. Plots of ΔG_1^{o} versus the logarithm of the molal concentration, log m_{D}, of AR88 for the first step of the DTA–AR88 complex formation in TX100 solutions of different concentrations at different temperatures. 1: 5.0×10^{-3} mol/kg TX100, 2: 1.0×10^{-2} mol/kg TX100, 3: 5.0×10^{-2} mol/kg TX100; —: 15 °C, - - - -: 25 °C, · · ·: 35 °C.

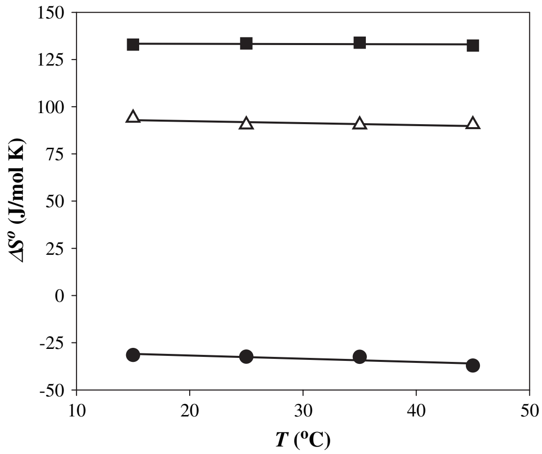

Fig. 6. Plots of ΔS_1^{o} versus T for the first step of the DTA–AR88 and DTA–TX100 micelle complexes formation in binary and three-component mixtures. -●-●-: DTA–AR88 in 1.0×10^{-4} mol/kg AR88, -■-■-: DTA–TX100 micelle in 1.0×10^{-2} mol/kg TX100, -△-△-: DTA–AR88 in the mixture of 1.0×10^{-4} mol/kg AR88 and 1.0×10^{-2} mol/kg TX100.

irrespective of the dispersive forces, which prevail in binding of DTA cations to AR88 anions, the hydrophobic interactions play an important role in DTA–AR88 complex formation in the presence of TX100 micelles. In this case the total interaction process is entropy-driven. A very logical explanation for these results can be that the DTA–AR88 complexes are solubilized in the TX100 micelles. In this case the breaking of the structured water surrounding the hydrophobic groups of DTA and AR88 can strongly increase the hydrophobic contribution to the value of ΔS_1^o. These results lead to the conclusion that added TX100 to the mixture of DTA and AR88 strongly affects the mode as well as the strength of the intermolecular interactions which act between the dye and surfactants present in the solution.

4. Conclusion

The results of the thermodynamic investigations of dye–surfactant interactions in different conditions present an opportunity to discuss the mode and the strength of intermolecular interactions which act between different species in solutions. It was observed that the presence of TX100 micelles causes a change in environment, which strongly affects the tendency of DTA–AR88 complex formation. The binding energy of DTA to AR88 is much lower in the presence of TX100 than in the absence of TX100. The addition of TX100 converts the DTA to AR88 binding process from exothermic to endothermic. Since the value of $T\Delta S_1^o$ for DTA–AR88 complex formation in TX100 solution is positive and much greater than ΔH_1^o, this process is entropy controlled.

Acknowledgements

This work was supported by the Ministry of High Education, Science and Technology of Slovenia.

References

[1] Simončič B, Špan J. A study of dye–surfactant interactions. Part 1. Effect of chemical structure of acid dyes and surfactants on the complex formation. Dyes and Pigments 1998;36(1):1–14.

[2] Bračko S, Špan J. Anionic dye–cationic surfactant interactions in water–ethanol mixed solvent. Dyes and Pigments 2001;50(1): 77–84.

[3] Navarro A, Sanz E. Chemical interaction between nonionic surfactants and an acid dye. Journal of Colloid and Interface Science 2001;237(1):1–5.

[4] Oakes J, Gratton P, Dixon S. Solubilisation of dyes by surfactant micelles. Part 3: a spectroscopic study of azo dyes in surfactant solutions. Coloration Technology 2003;119(5):301–6.

[5] Gokturk S, Tuncay M. Dye–surfactant interaction in the premicellar region. Journal of Surfactants and Detergents 2003; 6(4):325–30.

[6] Sabate R, Estelrich J. Determination of micellar microenvironment of pinacyanol by visible spectroscopy. Journal of Physical Chemistry B 2003;107(17):4137–42.

[7] Forte-Tavčer P. Interactions between some anionic dyes and cationic surfactants with different alkyl chain length studied by the method of continuous variations. Dyes and Pigments 2004; 63(2):181–9.

[8] Ghoreishi SM, Nooshabadi MS. Electromotive force studies about some dyes–cationic surfactants interactions in aqueous solutions. Dyes and Pigments 2005;65(2):117–23.

[9] Behera PK, Mohapatra S, Patel S, Mishra BK. Dye–surfactant interaction: solubilisation of styryl pyridinium dyes of varying alkyl chain in alfa-olefinic sulfonate and linear alkyl benzene sulfonate solutions. Journal of Photochemistry and Photobiology A – Chemistry 2005;169(3):253–60.

[10] Simončič B, Kert M. A study of anionic dye–cationic surfactant interactions in mixtures of cationic and nonionic surfactants. Dyes and Pigments 2002;54(3):221–37.

[11] Fabios R, Sicilia MD, Rubio S, Perez-Bendito D. Surfactant to dye binding degree-based methodology for the determination of ionic amphiphilic compounds. Analytical Chemistry 2003;75(21):6011–6.

[12] Kartal C, Akbas H. Study on the interactions of anionic dye–nonionic surfactants in a mixture of anionic and nonionic surfactants by absorption spectroscopy. Dyes and Pigments 2005; 65(3):191–5.

[13] Akbas H, Kartal C. Spectrophotometric studies of anionic dye–cationic surfactant interactions in mixture of cationic and nonionic surfactants. Spectrochimica Acta Part A – Molecular and Biomolecular Spectroscopy 2005;61(5):961–6.

[14] Simončič B, Papež V. Potentiometric study of intermolecular interactions in cationic–nonionic mixed surfactant systems. Textile Research Journal 2000;70(5):454–9.

[15] Akbas H, Iscan M, Sidim T. Composition of mixed anionic/ nonionic surfactant micelles. Journal of Surfactants and Detergents 2000;3(1):77–80.

[16] Varade D, Mody S, Ankleshwaria H, Bahadur P. Mixed surfactant systems. Part 1: micelle formation from mixtures of polyoxyethylene *t*-octylphenol and cationic surfactants. Tenside Surfactants Detergents 2003;40(1):46–51.

[17] Wydro P, Paluch M. Surface properties of cationic–nonionic mixed surfactant systems. Colloids and Surfaces A – Physicochemical and Engineering Aspects 2004;245(1–3):75–9.

[18] Rossoti FJC, Rossotti H. The determination of stability constants and other equilibrium constants in solution. New York: McGraw-Hill Book Company; 1961. p. 1–188.

[19] Cutler SG, Meares PJ, Hall DG. Surfactant-sensitive polymeric membrane electrodes. Electroanalytical Chemistry 1977;85: 145–8.

[20] Simončič B, Špan J, Vesnaver G. Acid Red 88 dye anion-selective electrode. Dyes and Pigments 1994;25:69–78.

[21] Benrraou M, Zanna R, Varokui R, Pefferkorn E. Study of the interaction between dodecyltrimethylammonium bromide and poly(maleic acid-co-alcyl vinyl ether) in aqueous solution by potentiometry and fluorescence probing. The Journal of Physical Chemistry 1992;96(3):1468–75.

[22] Jha R, Ahluwalia JC. Thermodynamics of micellization of Triton X-100 in aqueous ethylene glycol solutions. Journal of Physical Chemistry 1991;76(20):7782–4.

[23] Morf WE. The principles of ion-selective electrodes and of membrane transport. Budapest: Akademiai Kiado; 1981. p. 1–120.

[24] Bhattacharya SC, Das H, Moulik SP. Visible and flourescence spectral studies on the interaction of safranine T with surfactant

micelles. Journal of Photochemistry and Photobiology A – Chemistry 1993;74(2–3):239–45.

[25] Klotz IM. Introduction to biomolecular energetics: including ligand–receptor interactions. New York: Academic Press; 1986. p. 103–33.

[26] Moore WJ. Physical chemistry. London: Longman Scientific and Technical; 1992.

[27] Gurney RW. Ionic processes in solution. New York: McGraw-Hill; 1953.

[28] Kauzmann W. Some factors in the interpretation of protein denaturation. Advances in Protein Chemistry 1959;14:1–63.

[29] Robinson RA, Stokes RH. Electrolyte solutions. London: Butterworths; 1959.

[30] Mukerjee P, Grosh AK. Thermodynamic aspects of the self-association and hydrophobic bonding of Methylene Blue. A model system for stacking interactions. Journal of the American Chemical Society 1970;92:6419–24.

[31] Vidulich GA, Evans DF, Kay RL. The dielectric constant of water and heavy water between 0 and 40 °. Journal of Physical Chemistry 1967;71:656–62.

[32] Simončič B, Špan J. A study of dye–surfactant interactions. Part 3. Thermodynamics of the association of C.I. Acid Orange 7 and cetylpyridinium chloride in aqueous solutions. Dyes and Pigments 2000;46:1–8.

[33] Bračko S. Conductometric study of interactions between anionic azo bye and some cationic surfactants. Ph.D. Thesis. Ljubljana, Faculty of Natural Sciences and Engineering; 1997.

[34] Panda AK, Chakraborty AK. Interaction of mixed surfactants with bacterial lipopolysaccharide. Journal of Colloid and Interface Science 1998;203:260–4.

[35] Gharibi H, Jalili S, Rajabi T. Electrochemical studies of interaction between cetyltrimethylammonium bromide and α-, β-cyclodextrins at various temperature. Colloids and Surfaces A: Physicochemical and Engineering Aspects 2000;175:361–9.